A Model System to Provide a Good in Vitro Simulation of Biological Mineralization

ARTICLE *in* CRYSTAL GROWTH & DESIGN · JANUARY 2004

Impact Factor: 4.89 · DOI: 10.1021/cg034066s

3 AUTHORS, INCLUDING:

Sergey V. Dorozhkin
N/A
179 PUBLICATIONS **3,991** CITATIONS

SEE PROFILE

CRYSTAL GROWTH & DESIGN
2004
VOL. 4, NO. 2
389−395

A Model System to Provide a Good in Vitro Simulation of Biological Mineralization

Sergey V. Dorozhkin,* Elena I. Dorozhkina, and Matthias Epple

Solid State Chemistry, Faculty of Chemistry, University of Bochum, D-44780 Bochum, Germany

Received April 24, 2003; Revised Manuscript Received July 18, 2003

ABSTRACT: The in vivo process of biological mineralization can be successfully simulated in vitro by a slow crystallization of a nonstoichiometric carbonated apatite from revised simulated body fluid (rSBF) carried out in a constant-composition double-diffusion (CCDD) device under physiological conditions (temperature 37 °C, solution pH within 7.2−7.4). The substitution of an organic buffer (Hepes) by permanent carbon dioxide bubbling to keep the pH constant has no strong influence on the crystallization. By increasing the overall concentration, calcification can be easily induced on porous bioinert surfaces such as cellulose or cholesterol that normally cannot be coated with calcium phosphates from supersaturated solutions without additional promoters.

Introduction

According to the definition, biological mineralization (biomineralization) is the process of in vivo formation of inorganic compounds by living organisms.[1] In the case of mammals, most types of calcified tissues (both normal and pathological) consist of calcium phosphates, mainly of so-called "biological apatite".[1−3] This is a nonstoichiometric, poorly crystalline carbonated apatite (synonym: dahllite; approximate chemical formula $(Ca,Mg,Na)_{10-x}(HPO_4,CO_3)_x(PO_4)_{6-x}(OH,CO_3)_{2-x}{\cdot}yH_2O$, where $0 < x < 2$ containing water, sodium, magnesium, strontium as well as minor amounts of other chemical elements.[2,4]

Chemical analysis of the blood serum of mammals for inorganic ions was done many times,[5,6] and after comparison with the solubility diagram of calcium phosphates in aqueous solutions,[2,4] the serum was found to be supersaturated with respect to precipitation of hydroxyapatite (HA) $Ca_{10}(PO_4)_6(OH)_2$. The crystal structure and other properties of biological apatite were found to be rather similar to those of a nonstoichiometric carbonated apatite.[1−3] Therefore, the in vivo processes of normal and pathological mineralization were often simulated in vitro by chemical precipitation of a nonstoichiometric and poorly crystalline HA.

The easiest way of chemical preparation of calcium phosphates consists of mixing of aqueous solutions containing calcium and phosphate ions.[2,4] However, such type of crystallization gives the precipitates with properties (chemical composition, Ca/P ratio, crystallinity, particle size, etc.) different from those of biological apatite.[7−10] This can be explained by the following differences between in vivo and in vitro crystallization conditions:

(i) In vitro crystallization from supersaturated aqueous solutions normally occurs at permanently depleting concentrations of calcium and phosphate, while the concentrations of these ions are kept strictly constant during biological mineralization (the same is valid for the solution pH);

(ii) Chemical crystallization is a fast process (time scale of minutes and hours), while the biological process is usually slow (time scale of weeks to years);

(iii) Many organic, biological, and polymeric compounds are present in biological liquids (blood plasma, serum, saliva). Each of these compounds can have an influence (either positive or negative) on the in vivo crystallization of calcium phosphates.

The first difference between the in vivo and in vitro crystallization conditions can be overcome by using continuous crystallization methods. For example, the precipitation of a bone-like apatite can be performed by placing a substrate into a continuous flow of a supersaturated solution.[11,12] Another way consists of using a constant-composition (CC) technique. Initially, this technique allowed the solution pH only to be kept constant,[13,14] but later, after ion-selective electrodes for calcium became available, the dual CC technique was introduced.[15,16] However, having been designed to study the fast process of chemical crystallization from supersaturated solutions, the CC technique is not well suited to simulate the slow process of biological mineralization. Nevertheless, some attempts were reported.[17]

The second difference can be overcome by a restrained diffusion in a double-diffusion (DD) crystallization device. To do so, a permeable membrane (e.g., collagen,[18−20] dialysis membrane,[21] or polyester[22]) separates two solutions containing calcium and phosphate, respectively, from each other. The ions slowly diffuse from the opposite sides of the membrane to meet in the center where crystallization occurs. This method strongly reduces the crystallization rate, making the conditions more similar to those present in vivo. Similarities between the precipitated calcium phosphates and human enamel were found as a result.[20,21] However, as the crystallization proceeds the solutions surrounding the crystallization sites are permanently depleted. Therefore, the crystallization rate also decreases, unlike in biological mineralization.

Recently, we suggested a way to overcome the above limitations of the CC and DD techniques by combining

* To whom correspondence should be addressed. Present address: Nicol Hall, Queen's University, 60 Union Street, Kingston, ON K7L 3N6, Canada; phone: +1 613-533-6000, ext: 77-542; fax: +1 613-533-6610; e-mail: sd21@post.queensu.ca.

10.1021/cg034066s CCC: $27.50
Published on Web 01/13/2004

Table 1. Ion Concentrations of Human Blood Plasma and Different SBF Solutions, mM

	Na^+	K^+	Ca^{2+}	Mg^{2+}	Cl^-	HCO_3^-	HPO_4^{2-}	SO_4^{2-}	pH	NaN_3, g L^{-1}	buffer[c]
human blood plasma	142.0	5.0	2.5	1.5	103.0	27.0	1.0	0.5	7.25−7.40		
standard SBF[25]	142.0	5.0	2.5	1.5	147.8[a]	4.2	1.0	0.5	7.40 ± 0.01		50.0 mM (tris)
synthetic body fluid[26]	142.0	5.0	2.5	1.5	125.0[a]	27.0	1.0	0.5	7.40 ± 0.01		50.0 mM (tris)
revised SBF (rSBF)[27−29]	142.0	5.0	2.5	1.5	103.0	27.0	1.0	0.5	7.40 ± 0.01		∼12 g L^{-1} (Hepes)
4 times rSBF-Ca	**568.0**[b]	**20.0**	**20.0**	**12.0**	**412.0**			**2.0**	**7.40 ± 0.01**	**0.1**	
4 times rSBF-PO_4	**568.0**[b]	**20.0**			**412.0**	**216.0**	**8.0**	**2.0**	**7.35 ± 0.03**	**0.1**	**∼80 g L^{-1} (Hepes)**
Ca-stock solution	568.0[b]	20.0	40.0	24.0	412.0			2.0	7.40 ± 0.01	0.1	
PO_4-stock solution	568.0[b]	20.0			412.0	432.0	16.0	2.0	∼10	0.1	

[a] Not considering 50 mM of chloride added with the tris/HCl buffer. [b] Contains extra 1.5 mM of sodium due to presence of NaN_3. [c] *tris* = tris-hydroxymethyl-aminomethan. Hepes = 2-(4-(2-hydroxyethyl)-1-piperazinyl)ethane sulfonic acid.

both of them into a constant-composition double-diffusion (CCDD) device. The device fastens together the advantages of both techniques, i.e., a slow crystallization (by double-diffusion) combined with constant solution compositions.[23,24]

The influence of many compounds present in the human body cannot be simulated easily. The best way would be to perform experiments using natural liquids (blood serum, saliva, lymph, etc.), but this is not easy for obvious reasons. To simplify the task, various biomimetic solutions were developed, and the so-called "simulated body fluid" (SBF) (This abbreviation is also used for a "synthetic body fluid".[26]) introduced by Kokubo et al. is the best known among them.[25] It is a metastable aqueous solution (supersaturated by calcium and phosphate with respect to the precipitation of HA) containing inorganic ions in concentrations nearly equal to those in human blood plasma (Table 1). However, as mentioned in Table 1, the standard SBF, first, contains the tris/HCl buffer, and, second, the concentration of hydrogencarbonate (4.2 mM) is only a fraction of that in blood plasma (27 mM).[25]

The problem of a low concentration of hydrogencarbonate ions has recently been overcome by first introducing a "synthetic body fluid"[26] and later a revised SBF (rSBF)[27] (Table 1). Due to the chemical similarity with human blood plasma, rSBF currently seems to be the best simulating solution. However, it contains Hepes buffer, and it loses CO_2 in open vessels.[27] Therefore, experiments with rSBF were performed in closed vessels only.[28,29]

The goal of this paper is to introduce a model system that is able to provide a good in vitro simulation of biological mineralization by combining the great advantages of the CCDD device with the chemical similarity of rSBF to human blood plasma.

Experimental Section

The principal design of the CCDD device is shown in Figure 1. The CCDD device consists of two thermostated glass vessels of 250 mL each. A porous membrane clamped between the vessels separates the solutions from each other (Figure 1).

Each of the vessels works as an independent CC device, equipped with a pH electrode and a peristaltic pump transporting solutions of HCl with concentrations of 0.5 and 0.05 M, respectively. In addition, in the calcium vessel (right vessel in Figure 1) there is a calcium selective electrode (model 97−20 *ionplus*, Orion Inc.). A third pump adds a stock solution of calcium. As the concentration of hydrogen phosphate cannot be continuously monitored, we made an assumption on the precipitation of stoichiometric HA. Thus, the consumption of hydrogen phosphate in left vessel of the CCDD device can be approximated if the consumption of calcium is known (note, that in reality, a nonstoichiometric, bone-like carbonated

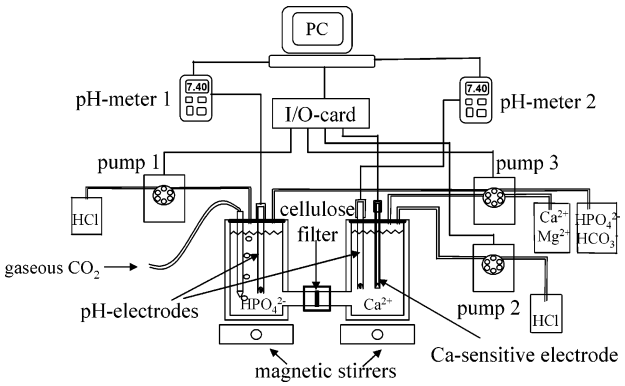

Figure 1. The principal scheme of the CCDD device. A tube with a cellulose filter inside connects two thermostated glass vessels. Two pH meters continuously monitor the pH in each vessel. A calcium-selective electrode continuously monitors the calcium concentration in the right vessel. Three peristaltic pumps perform the addition of the calcium + magnesium and hydrogenphosphate + hydrogencarbonate stock solutions, as well as of HCl for pH adjustment. Permanent bubbling of CO_2 is made into the left vessel.

apatite, containing admixtures of other ions, is precipitated from SBF,[11,12,25−29] but this cannot be quantitatively taken into account). Therefore, the stock solutions of calcium and phosphate ions in a concentration ratio of 10:6 are simultaneously added into the CCDD device by one multichannel peristaltic pump (Figure 1).[23,24]

We used ashless 589[3] filter paper (blue ribbon, Schleicher & Schuell, No. 300210) as an inert porous membrane and rSBF (Table 1) as a mineralizing solution. To avoid a possible growth of bacteria during the experiments, we added 0.1 g L^{-1} of NaN_3 to rSBF (Table 1). As rSBF mimics the chemical composition of human blood plasma, the crystallization rate is very small.[25−29] This would require long-time mineralization experiments. Some authors have addressed this problem by using SBF solutions containing 1.5 times the ionic concentrations of the standard SBF (so-called 1.5SBF).[28−31] We have extended this idea further and decided to work with solutions containing 4 times the ionic concentrations of rSBF. However, such a solution cannot be prepared in one vessel because crystallization would start during its preparation. For this reason, we prepared two solutions of 4 times rSBF: one of them contained the double concentration of calcium and magnesium ions but no hydrogen phosphate and hydrogen carbonate ions (4rSBF-Ca) and another one vice versa (4rSBF-PO_4). After mixing in equal amounts, 4rSBF-Ca and 4rSBF-PO_4 give rise to 4 times rSBF (Table 1).

For 4rSBF-PO_4, the pH was initially adjusted by addition of Hepes[27] (Table 1) to pH = 7.5 followed by further adjustment by continuous bubbling of CO_2 to pH = 7.35 ± 0.03. For 4rSBF-Ca, the pH was adjusted by NaOH to pH = 7.35 ± 0.03.

The stock solutions of calcium and phosphate contained the double amounts of calcium and magnesium, as well as hydrogen phosphate and hydrogen carbonate ions compared to 4rSBF-Ca and 4rSBF-PO_4 (Table 1). For the calcium stock solution, the pH was adjusted to 7.35 ± 0.03 also by NaOH,

but the solution pH of the phosphate stock solution was not adjusted and remained at about 10 (Table 1). This was necessary to keep the full amount of carbonate in the phosphate stock solution. All the solutions were prepared with reagents of pro analysi quality obtained from Merck and double-distilled water.

Permanent bubbling of gaseous CO_2 through the 4rSBF-PO_4 solution solved the problem of chemical instability of rSBF (loss of carbonate). We found that by adjusting of the CO_2 flow the solution pH of the 4rSBF-PO_4 solution could be kept with a precision of ±0.05 pH units (see below). The bubbling rate was about 0.5 mL s^{-1}.

The experiments were performed under physiological conditions (temperature 37.0 ± 0.2 °C and pH = 7.35 ± 0.05). Each experiment started with the addition of 70 mL of the 4rSBF-Ca and 4rSBF-PO_4 solutions into the corresponding glass vessels of the CCDD device and lasted for 6−7 days. After the experiment, the filter was removed, washed with deionized water, dried at 37 °C until a constant mass was reached, and weighed. The chemical and structural composition of the precipitates formed were studied by scanning electron microscopy (SEM; LEO 1530; gold sputtering) coupled with energy-dispersive X-ray (EDX) spectroscopy (ISIS, Link Analytical, Oxford Instruments), infrared (IR) spectroscopy (1720X, Perkin-Elmer), and X-ray diffraction (XRD; D8 Advance, Bruker AXS; Cu Kα radiation). However, the amount of the precipitates (about 10−15 mg after one week) was too small to determine its chemical composition by chemical analysis.

After the experiments, calcium and magnesium concentrations in the 4rSBF-Ca solution were determined. Titration of calcium was made by 0.01 M EDTA at pH = 12 with calcon carbonic acid (Merck) as indicator. Later, the indicator was oxidized by H_2O_2 and titration of magnesium was performed at pH = 8.5 with Eriochrom black T (Merck) as indicator. In the 4rSBF-PO_4 solution, the concentration of phosphate was determined photometrically via formation of the blue ammonium phosphate−molybdate complex. Hydrogen carbonate was determined gravimetrically by $BaCO_3$ precipitation at pH > 13.0 (an excess of a saturated solution of $Ba(OH)_2$ was added to the 4rSBF-PO_4 solution; the precipitate was collected, dried, and weighed).

To illustrate the great advantages of the combination of a CCDD device with rSBF, three sets of experiments were performed under conditions slightly different from those described above. The first set was done as above but with Hepes-free 4rSBF-PO_4 (solution pH was adjusted to 7.4 solely by CO_2 bubbling). The second one was carried out with solutions of 6 times rSBF (6rSBF-Ca and 6rSBF-PO_4, respectively). The third set was made with 6 times rSBF and a porous pellet of cholesterol (pores were introduced by leaching out initially present NaCl crystals) was used instead of the cellulose filter.

Results

Stability Parameters of the CCDD Device. Typical stability parameters of the CCDD device containing 4rSBF-Ca and 4rSBF-PO_4 solutions can be seen in Figure 2. As shown in plot 1, the signal from the calcium selective electrode was about 9.5 ± 0.5 mV during the mineralization experiments. The calcium concentration was kept constant with a precision of 10% (Table 2).

However, the sensitivity of the calcium selective electrode was limited (seen as noise and drift). This probably happened due to the presence of magnesium and sodium in 4 times rSBF. According to the electrode manual supplied by the manufacturer, both ions may cause measurement errors for calcium determination. To overcome this problem, the theoretical concentrations for calcium and phosphate were introduced into the software as described below.

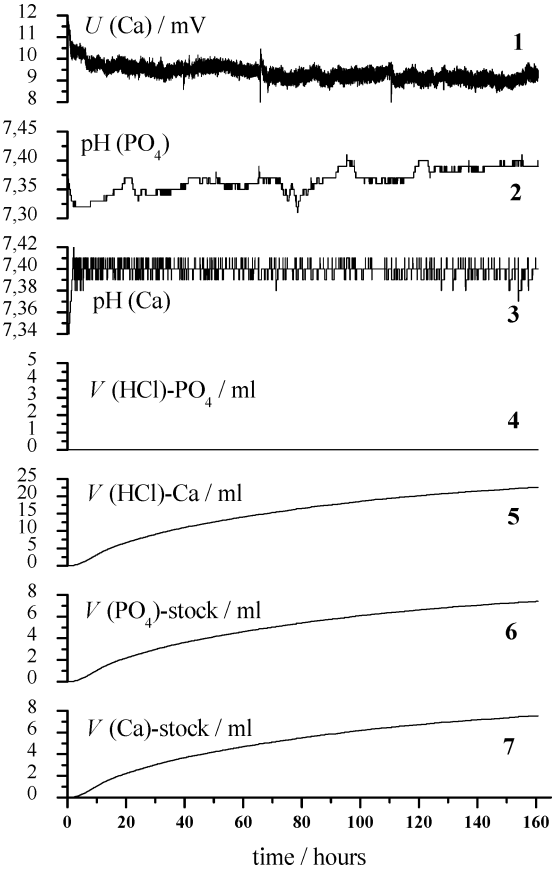

Figure 2. Stability parameters of the CCDD device: 1 − potential of calcium selective electrode; 2 − pH in the phosphate vessel; 3 − pH in the calcium vessel; 4 − volume of 0.5 M HCl added into the phosphate vessel to keep the pH constant; 5 − volume of 0.05 M HCl added into the calcium vessel to keep the pH constant; 6 − volume of phosphate stock solution added into the phosphate vessel to keep the concentration of phosphate and carbonate constant; 7 − volume of calcium stock solution added into the calcium vessel to keep the concentration of calcium and magnesium ions constant.

As shown in plots 2 and 3, in both vessels of the CCDD device the solution pH was kept constant but with different precision: 7.35 ± 0.05 in the phosphate vessel and 7.40 ± 0.01 in the calcium vessel. The former value was adjusted by the flow of CO_2 permanently bubbling through the 4rSBF-PO_4 solution, while the latter value was adjusted by the addition of 0.05 M HCl (plot 5). The flow of CO_2 was chosen to keep the solution pH of 4rSBF-PO_4 slightly below the desired value of 7.40 (plot 2). Therefore, the addition of HCl stock solution to the phosphate side was never triggered (plot 4).

Plots 6 and 7 represent the amounts of calcium and phosphate stock solutions (16rSBF each for $Ca^{2+} + Mg^{2+}$ and $HPO_4^{2-} + HCO_3^-$, respectively) added to both vessels to keep the concentrations of these ions constant. Due to the mentioned instability of the calcium-selective electrode, the theoretical calcium concentration in the calcium vessel was permanently calculated based on the initial concentration of calcium ions, initial volume of the 4rSBF-Ca solution and the dilution effect by the addition of HCl and calcium stock solutions. The stock solution of calcium was added only if two conditions were simultaneously fulfilled: (i) the theoretical value of calcium was less than the desired value of 20 mM (see Table 1) and (ii) the calcium-selective electrode

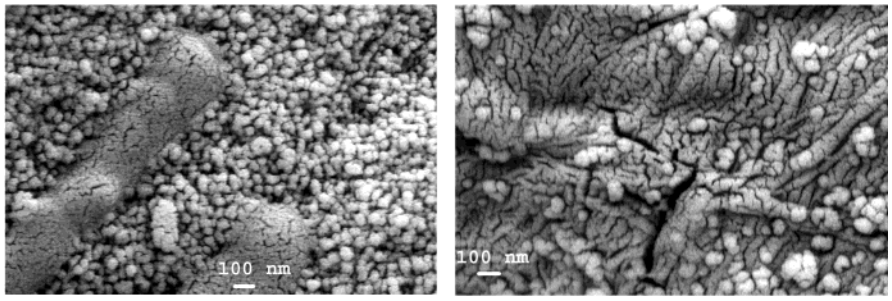

Figure 3. Scanning electron micrographs of the precipitates from 4 times rSBF solutions formed onto both sides of the cellulose filter after 7 days of the experiment: a − calcium side, b − phosphate side. Magnification: 100000×. Bar: 100 nm. Note that both sides are completely covered by calcium phosphate with the cellulose fiber microstructure being still visible on the phosphate side (b) below the spherical crystallites.

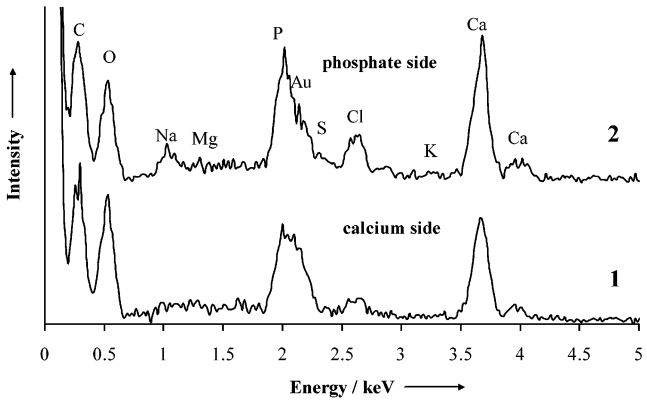

Figure 4. Energy-dispersive X-ray spectroscopy of the precipitates from 4 times rSBF solutions on the cellulose filter.

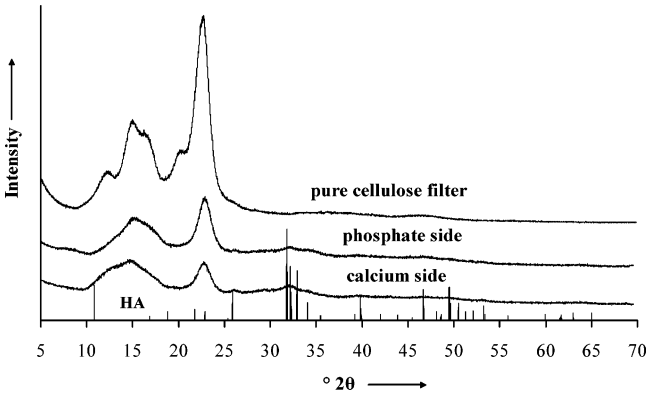

Figure 5. X-ray diffraction patterns of the precipitates from 4 times rSBF solutions on the cellulose filter. The diffraction patterns of the initial cellulose filter (upper pattern) and well crystallized HA (lower pattern) are given for comparison.

showed a decreased electrical potential compared to the initial value.

The results of the chemical analysis of the initial and final solutions are summarized in Table 2. One can see that during the experiments in the CCDD device the concentrations of the ions participating in the crystallization remained mostly constant.

Precipitates of Calcium Phosphates from rSBF. Typical precipitates obtained in the CCDD device from 4 times rSBF are shown in Figure 3 (here and below cracks are due to dehydration during samples preparation). The crystals are very similar on both sides of the cellulose filter and form beadlike aggregates of 50−100 nm in diameter similar to those precipitated from synthetic body fluid.[26] The surface is fully covered with calcium phosphate on both sides. This can be shown by EDX and by comparison with the fiberlike structure of the pure filter.

As shown in Figure 4, the precipitates consist of calcium phosphate with minor incorporations of sodium and chloride. The strong peak of gold is due to sputtering, while that of carbon may have two different origins: from cellulose and from carbonates coprecipitated with phosphates. Magnesium, sulfur, and potassium are present in traces only: the peaks of these elements are hardly distinguishable from the background. Small amounts of all these ions are present in bones, teeth, and other calcified tissues of mammals.[1,2,4] Therefore, we confirm the results of the rSBF inventors[27−29] on the chemical similarity between the biologically formed calcified tissues and precipitates formed from rSBF.

XRD results are shown in Figure 5. The precipitates are of very poor crystallinity. Due to overlapping with the strong diffraction pattern of the cellulose filter, the diffraction patterns of the precipitates cannot be resolved in the range of 5−25 °2θ. However, on both sides of the mineralized filter the diffraction peaks of cellulose have lower intensities compared to the unmineralized filter. This indicates a diminution of the X-ray beam due to the presence of calcium phosphate on the surface. The diffraction pattern of well-crystallized HA is shown for comparison.

The results of IR spectroscopy are shown in Figure 6. The bands at 3400 and 1634 cm^{-1} are due to the either adsorbed or incorporated water, and those at 1470 and 1420 cm^{-1} are the specific absorption bands of

Table 2. Chemical Analysis of 4 Times rSBF Solutions before and after the Mineralization Experiments (one week) in mM

calcium side				phosphate side			
Ca^{2+}		Mg^{2+}		HPO_4^{2-}		HCO_3^-	
before	after	before	after	before	after	before	after
20.1 ± 0.3	19.8 ± 0.5	11.7 ± 0.5	13.5 ± 1.5	7.8 ± 0.4	8.2 ± 0.4	220 ± 10	230 ± 15

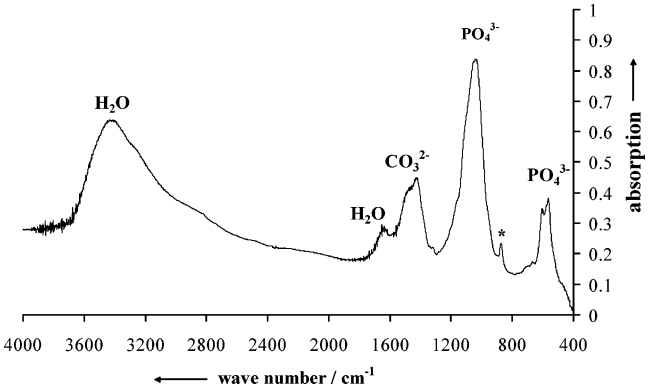

Figure 6. IR spectra of the precipitates formed on the cellulose filter from 4 times rSBF solutions. The band marked by an asterisk (at 875 cm^{-1}) corresponds to either CO_3^{2-} or HPO_4^{2-}.

B-type carbonated apatite (i.e., ions of carbonate are in the places of phosphate ions). The bands at 1030, 585, and 560 cm^{-1} are specific for phosphate ions, and the band at 868 cm^{-1} corresponds to either B-type carbonated apatite or to the HPO_4^{2-} ion.[2,4] All IR bands are broad, indicating a poor crystallinity. These results confirm that the precipitates formed in the CCDD device from 4 times rSBF solutions consist of a poorly crystallized, nonstoichiometric carbonated apatite.

SEM pictures of the precipitates formed on the cellulose filter from a Hepes-free 4 times rSBF, 6 times rSBF containing Hepes, as well as the precipitates formed on the surface of porous pellets of cholesterol are shown in Figures 7−9, respectively. Note that the surface is in all cases completely covered by calcium phosphate, as in Figure 3.

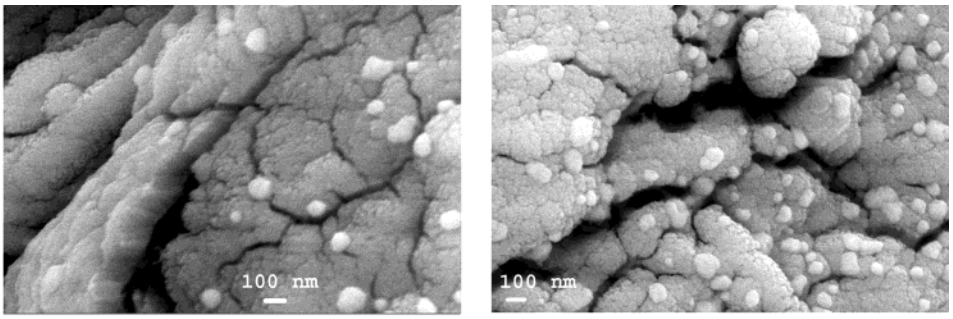

Figure 7. Scanning electron micrographs of the precipitates from 4 times Hepes-free rSBF solutions (containing 8 times 52 mM of HCO_3^-) on both sides of the cellulose filter after 7 days of the experiment: a − calcium side, b − phosphate side. The pH was adjusted by permanent bubbling of CO_2. Magnification: 100000×. Bar: 100 nm.

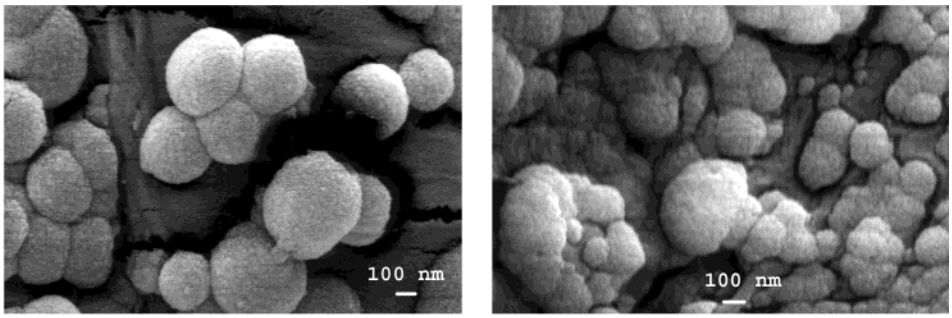

Figure 8. Scanning electron micrographs of the precipitates from 6 times rSBF solutions formed on both sides of the cellulose filter after 7 days of the experiment: a − calcium side, b − phosphate side. Magnification: 100000×. Bar: 100 nm.

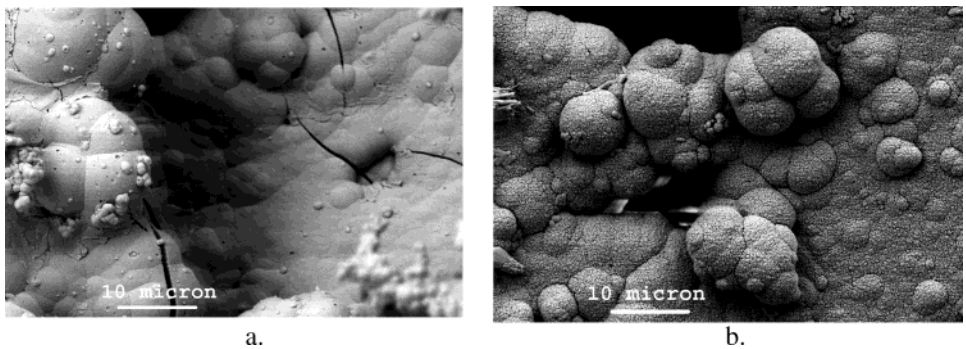

Figure 9. Scanning electron micrographs of the precipitates from 6 times rSBF solutions formed on both sides of a porous cholesterol pellet after 7 days of the experiment: a − calcium side, b − phosphate side. Magnification: 2000×. Bar: 10 μm.

For precipitates from a Hepes-free 4 times rSBF, the amount of the precipitates was not enough to make IR investigations. XRD revealed an even poorer crystallinity compared to Figure 5, while EDX detected a higher intensity for the peak of carbon compared to Figure 4 (probably due to the filter). Analysis of the precipitates formed in 6 times rSBF containing Hepes by XRD, IR, and EDX gave the same results as in Figures 4−6. In the case of the precipitates formed from 6 times rSBF on cholesterol pellets, IR was unsuccessful due to impossibility to separate calcium phosphate from cholesterol, XRD revealed overlapping of weak diffraction peaks of calcium phosphate with strong ones of cholesterol (which complicated the comparison with Figure 5), while EDX spectra of the precipitates were similar to those shown in Figure 4.

Discussion

Many experiments with standard SBF (not rSBF!) solutions were reported and the precipitates were found to consist of poorly crystallized, nonstoichiometric, sodium-, magnesium- and carbonate-containing apatite resembling that of human bone.[11,12,25,30−39] As expected, the chemical composition of the precipitates formed in rSBF under physiological conditions is even closer to bone mineral. From the chemical point of view, the precipitates formed in rSBF contain a higher amount of carbonates, a smaller amount of chlorides, and have a higher Ca/P molar ratio compared to those formed in SBF.[27−29] Surprisingly, no differences in crystal shape and sizes between the precipitates formed in SBF and rSBF were found: all of them consisted of small crystallites with needlelike morphology.[29] However, beadlike aggregates of 50−100 nm in sizes were precipitated from rSBF in our study (Figure 3). For better comparison of our data with those from references, the main particularities of our study are summarized below.

Solutions of rSBF that are kept in open vessels are known to lose part of carbonate, which results in increasing pH.[27] In our study, this problem has been overcome by permanent bubbling of gaseous CO_2. Previous researchers working with SBF[25,30−39] and rSBF[28,29] were unable to keep the solution pH and its composition strictly constant. Frequent renewal was the most common way to keep the solution composition approximately constant.[28,29,38,39] Recently, a continuous exchange of the solution was proposed by Vallet-Regi et al.,[11,12] but this study was performed before the development of rSBF. We presented a new way to address this problem by performing experiments in a CCDD device.[23,24] By this method, we have obtained beadlike precipitates (Figure 3) different from the needlelike crystals precipitated from rSBF under less controlled conditions.[29] Spherical particles of a bone-like apatite of 35−50 nm in size were also obtained by a "continuous addition type precipitation" from synthetic body fluid.[26] Biological apatite of bone consists of a platelike crystals of 50 × 25 × 4 nm in sizes,[1] which are close to the dimensions of our precipitates. The differences in crystal shapes between natural bone and the precipitates from rSBF can be explained by the presence of organic and biological compounds in human liquids.

An attempt to get rid of Hepes buffer which is present in rSBF for pH adjustment (Table 1) but not in blood plasma can be illustrated by comparison of Figures 3 and 7. A replacement of Hepes by permanent bubbling of CO_2 gives no strongly different crystal morphologies. The results of chemical analysis revealed that after the solution pH = 7.35 ± 0.03 was reached, the Hepes-free 4rSBF-PO_4 solution contained 8 times 52 mM of HCO_3^- ions instead of the desired 8 times 27 mM (see Table 1). This deviation from the biomimetic concentration ratio could be addressed by regulation of the CO_2 bubbling rate to yield the desired carbonate concentration in solution without additional buffer, but apparently, this variation in carbonate concentration has no decisive influence on the crystallization.

The previous investigators dealt with either 1 time or 1.5 times SBF[11,12,25,30−39] and rSBF,[28,29] and only few papers on mineralization experiments in 2 times SBF were published.[38] Higher concentrated solutions cannot be prepared because the precipitation starts during preparation. The advantage of the CCDD device over a continuous exchange of SBF[11,12] is the separation of calcium and magnesium cations from anions of hydrogenphosphate and hydrogencarbonate with up to 8 times the ionic concentrations of SBF and rSBF. This allows us to influence the crystallization kinetics and extends the applicability of both solutions. Our experiments with 6 times rSBF containing Hepes resulted in larger crystallites (Figures 3 and 8) as well as greater amounts of the precipitates (12 ± 2 mg vs 32 ± 3 mg after one week for 4 and 6 times rSBF, respectively). However, no differences were found by EDX, XRD, and IR; therefore, the "chemistry" of the crystallites is still the same.

Some compounds (e.g., cellulose,[30,34,35] collagen,[36] and poly(ethylene terephthalate) (PET)[37−39]) were found to be rather bioinert and not to promote apatite formation on their surface from 1.5 times SBF. To increase the bioactivity of cellulose, it was suggested to either phosphorylated it by phosphoric acid,[34,35] or to add citric acid to 1.5 times SBF.[36] To increase the bioactivity of PET, a pretreatment by sodium silicate[37] or the presence of CaO−SiO_2-based glasses were suggested.[28,38,39] It can be claimed that the bioinertness of many compounds can be easily overcome by using 4 times rSBF (e.g., see Figure 3 for cellulose).

Using the CCDD device with 6 times rSBF, we have succeeded to precipitate a bone-like apatite on the surface of a porous pellet of cholesterol (Figure 9). It should be stressed that for the first time the precipitation of apatite onto cholesterol was achieved from aqueous solutions; the previous investigators crystallized apatite−cholesterol composites only from alcohol[40,41] (cholesterol is hydrophobic and only sparingly soluble in water). Thus, a combination of the CCDD device with rSBF can provide a new insight into the simulation of cardiovascular diseases.

Finally, further modifications of rSBF can be performed easily. The desired compounds normally present in human blood plasma (e.g., albumins, glucose, proteins, etc.) can be added into either one or both vessel(s) of the CCDD device and the influence of these compounds to precipitation of a bone-like apatite can be conveniently studied. The influence of magnesium, fluoride, and cholesterol on HA crystallization was published previously,[23,24] and the results were consis-

tent with references. Currently, the influence of glucose and bovine serum albumin added to rSBF is studied.

Conclusions

A combination of the CCDD device with rSBF is able to overcome three main differences between in vitro and in vivo crystallization conditions and to provide a good simulation of biological mineralization. This combination provides many additional opportunities to influence the crystallization kinetics making it faster or slower (therefore, less or more close to the in vivo conditions) where necessary. The latter can be performed by variation of solution concentrations, the presence or absence of biologically relevant additives, as well as by variation of the matrix and its porosity. This system can provide new insights by a successful simulation of both normal and pathological mineralization.

Acknowledgment. This work was supported by the Deutsche Forschungsgemeinschaft (DFG), Bonn, Germany, and the Fonds der Chemischen Industrie, Frankfurt/Main, Germany.

References

(1) Lowenstam, H. A.; Weiner, S. *On Biomineralization*; Oxford University Press: New York, 1989.
(2) LeGeros, R. Z. *Calcium Phosphates in Oral Biology and Medicine*; Karger: Basel, 1991.
(3) Tomazic, B. B. *Z. Kardiol.* **2001**, *90* (*Suppl. 3*), III/68−III/80.
(4) Elliot, J. C. *Structure and Chemistry of the Apatites and Other Calcium Orthophosphates*; Elsevier: Amsterdam, 1994; Vol. 18.
(5) Kupke, I. R.; Kather, B.; Zeugner, S. *Clin. Chim. Acta* **1981**, *112*, 177−185.
(6) Falch, D. K. *Scand. J. Clin. Lab. Invest.* **1981**, *41*, 59−62.
(7) Moreno, E. C.; Gregory, T. M.; Brown, W. E. *J. Res. Natl. Bur. Stand.* **1968**, *72A*, 773−787.
(8) Nancollas, G. H.; Mohan, M. S. *Arch. Oral Biol.* **1970**, *15*, 731−745.
(9) Blumenthal, N. C.; Posner, A. S. *Calcif. Tissue Res.* **1973**, *13*, 235−243.
(10) Eanes, E. D. *Calcif. Tiss. Res.* **1976**, *20*, 75−89.
(11) Izquierdo-Barba, I.; Salinas, A. J.; Vallet-Regi, M. *J. Biomed. Mater. Res.* **2000**, *51*, 191−199.
(12) Vallet-Regi, M.; Pérez-Pariente, J.; Izquierdo-Barba, I.; Salinas, A. J. *Chem. Mater.* **2000**, *12*, 3770−3775.
(13) Tomson, M. B.; Nancollas, G. H. *Science* **1978**, *200*, 1059−1060.
(14) Koutsoukos, P.; Amjad, Z.; Tomson, M. B.; Nancollas, G. H. *J. Am. Chem. Soc.* **1980**, *102*, 1553−1557.
(15) Ebrahimpour, A.; Zhang, J.; Nancollas, G. H. *J. Cryst. Growth* **1991**, *113*, 83−91.
(16) Tucker, B. E.; Cottell, C. M.; Auyeung, R. C.; Spector, M.; Nancollas, G. H. *Biomaterials* **1996**, *17*, 631−637.
(17) Nancollas, G. H.; Wu, W. *J. Cryst. Growth* **2000**, *211*, 137−142.
(18) Kniep, R.; Busch, S. *Angew. Chem.* **1996**, *108*, 2788−2791; Kniep, R.; Busch, S. *Angew. Chem. Int. Ed. Engl.* **1996**, *35*, 2624−2627.
(19) Busch, S.; Dolhaine, H.; DuChesne, A.; Heinz, S.; Hochrein, O.; Laeri, F.; Podebrad, O.; Vietze, U.; Weiland, T.; Kniep, R. *Eur. J. Inorg. Chem.* **1999**, 1643−1653.
(20) Busch, S.; Schwarz, U.; Kniep, R. *Chem. Mater.* **2001**, *13*, 3260−3271.
(21) Iijima, M.; Moriwaki, Y.; Takagi, T.; Moradian-Oldak, J. *J. Cryst. Growth* **2001**, *222*, 615−626.
(22) Schwarz, K.; Epple, M. *Chem. Eur. J.* **1998**, *4*, 1898−1903.
(23) Peters, F.; Epple, M. *Z. Kardiol.* **2001**, *90* (*Suppl. 3*), III/81−III/85.
(24) Peters, F.; Epple, M. *J. Chem. Soc., Dalton Trans.* **2001**, 3585−3592.
(25) Kokubo, T.; Kushitani, H.; Sakka, S.; Kitsugi, T.; Yamamuro, T. *J. Biomed. Mater. Res.* **1990**, *24*, 721−734.
(26) Tas, A. C. *Biomaterials* **2000**, *21*, 1429−1438.
(27) Kim, H. M.; Miyazaki, T.; Kokubo, T.; Nakamura, T. In *Bioceramics 13*; Giannini, S., Moroni, A., Eds.; Trans Tech Publ.: Switzerland, 2001; pp 192−195, 47−50.
(28) Kaneko, H.; Uchida, M.; Kim, H. M.; Kokubo, T.; Nakamura, T. In *Bioceramics 14*; Brown, S., Clarke, I. C., Williams, P., Eds.; Trans Tech Publ.: Switzerland, 2002; pp 218−220, 649−652.
(29) Kim, H. M.; Furuya, T.; Kokubo, T.; Miyazaki, T.; Nakamura, T. In *Bioceramics 14*; Brown, S., Clarke, I. C., Williams, P., Eds.; Trans Tech Publ.: Switzerland, 2002; pp 218−220, 621−624.
(30) Varma, H. K.; Yokogawa, Y.; Espinosa, F. F.; Kawamoto, Y.; Nishizawa, K.; Nagata, F.; Kameyama, T. *Biomaterials* **1999**, *20*, 879−884.
(31) Greish, Y. E.; Brown, P. W. *J. Biomed. Mater. Res.* **2000**, *52*, 687−694.
(32) Takadama, H.; Kim, H. M.; Kokubo, T.; Nakamura, T. *J. Biomed. Mater. Res.* **2001**, *57*, 441−448.
(33) Marques, P. A. A. P.; Magalhaes, M. C. F.; Dorozhkin, S. V.; Correia, R. N. In *Bioceramics 13*; Giannini, S., Moroni, A., Eds.; Trans Tech Publ.: Switzerland, 2001; pp 192−195, 27−30.
(34) Mucalo, M. R.; Yokogawa, Y.; Toriyama, M.; Suzuki, T.; Kawamoto, Y.; Nagata, F.; Nishizawa, K. *J. Mater. Sci. Mater. Med.* **1995**, *6*, 597−605.
(35) Mucalo, M. R.; Yokogawa, Y.; Suzuki, T.; Kawamoto, Y.; Nagata, F.; Nishizawa, K. *J. Mater. Sci. Mater. Med.* **1995**, *6*, 659−669.
(36) Rhee, S. H.; Tanaka, J. *Biomaterials* **1999**, *20*, 2155−2160.
(37) Miyaji, F.; Kim, H. M.; Handa, S.; Kokubo, T.; Nakamura, T. *Biomaterials* **1999**, *20*, 913−919.
(38) Kim, H. M.; Kishimoto, K.; Miyaji, F.; Kokubo, T.; Yao, T.; Suetsugu, Y.; Tanaka, J.; Nakamura, T. *J. Biomed. Mater. Res.* **1999**, *46*, 228−235.
(39) Kim, H. M.; Kishimoto, K.; Miyaji, F.; Kokubo, T.; Yao, T.; Suetsugu, Y.; Tanaka, J.; Nakamura, T. *J. Mater. Sci. Mater. Med.* **2000**, *11*, 421−426.
(40) Hirsch, D.; Azoury, R.; Sarig, S. *J. Cryst. Growth* **1990**, *104*, 759−765.
(41) Hirsch, D.; Azoury, R.; Sarig, S.; Kruth, H. S. *Calcif. Tissue Int.* **1993**, *52*, 94−98.

CG034066S